Glaucoma-associated abnormalities in cortical activity during a visuocognitive task

Clementine Garric, Yannick Wamain, Jean-François Rouland, Quentin Lenoble

Title:

Glaucoma-associated abnormalities in cortical activity during a visuocognitive task: an exploratory study

Author names and affiliations:

Clémentine Garric[1] (PhD), Yannick Wamain[2] (PhD), Jean-François Rouland[3] (MD, PhD), Quentin Lenoble[1] (PhD)

[1] Univ. Lille, INSERM, CHU Lille, U1172 - LilNCog - Lille Neuroscience and Cognition, F-59000 Lille, France

[2] Univ. Lille, CNRS, CHU Lille, UMR 9193, SCALab, Sciences Cognitives et Sciences Affectives, F-59000 Lille, France

[3]Ophthalmology Department, Claude Huriez Hospital, University of Lille, F-59000 Lille, France

Corresponding Author:

Clémentine Garric (PhD), clementine.garric@u-paris.fr

https://orcid.org/0000-0002-3963-9800

Publication work affiliation: Univ. Lille, INSERM, CHU Lille, U1172 - LilNCog - Lille Neuroscience and Cognition, F-59000 Lille

Present affiliation: CNRS, INCC, UMR 8002, Université Paris Cité, F-75006 Paris, France.

Co-authors:

yannick.wamain@univ-lille.fr
jean-francois.rouland@chu-lille.fr
quentin.lenoble@univ-lille.fr

Conflict of Interest

None of the authors have potential conflicts of interest to be disclose.

Acknowledgments and Funding statement

The lead authors received a PhD fellowship from the Centre Hospitalier Universitaire de Lille and the Région Hauts de France. The authors thank the Ophthalmology Department at Claude Huriez Hospital (Lille, France) for hosting the experimental sessions.

Abbreviations

ANOVA: analysis of variance

CR: correct rejection

dB: decibel

EEG: electroencephalography

ERP: event-related potential

FA: false alarm

FIR: finite impulse response

H: hit

Log CS: Logarithm of the Contrast Sensitivity

LogMAR : Logarithm of the Minimum Angle of Resolution

LPF: low-pass filter

MD: mean deviation

NF: non-filtered

POAG: primary open-angle glaucoma

VEP: visual evoked potential

Abstract

Objective: To investigate neurophysiological dynamics during a visuocognitive task in glaucoma patients vs. healthy controls.

Methods: Fifteen patients with early-stage primary open-angle glaucoma (POAG) and fifteen age-matched healthy participants underwent a "go/no-go" task, monitored with electroencephalography (EEG). Participants had to semantically categorize visual objects in central vision, with animal or furniture as targets according to the experimental block.

Results: Early visual processing was delayed by 50 milliseconds (ms) in patients with POAG compared to controls. The patients displayed a smaller difference between animal and furniture categorization during higher-level cognitive processing (at 400-600 ms). Regarding behavioral data, the groups differed in accuracy performance and decision criterion. As opposed to the control group, patients did not display facilitation and a higher accuracy rate for animal stimuli. However, patients maintained a consistent decision criterion throughout the experiment, whereas controls displayed a shift towards worse decision criteria in furniture trials, with higher error rate.

Conclusions: The comparative analysis of behavioral and neurophysiological data revealed in POAG patients a delay in early visual processing, and potential high-level cognitive compensation during late, task-dependent activations.

Significance: To our knowledge, our findings provide the first evidence of modification in cognitive brain dynamics associated with POAG.

Key Words

Glaucoma, Vision Loss, EEG, Cognition, Plasticity

1. Introduction

Primary open-angle glaucoma (POAG) is a complex visual disorder defined clinically by optic nerve degeneration and a progressive loss of peripheral and then central vision. Brain imaging studies have shown that damage to the optic nerve not only alters the patient's sensory functions but also impacts the central nervous system's fine-scale structure (Arrigo et al., 2021; Chen et al., 2013; Lawlor et al., 2018; Nucci et al., 2020; Nuzzi et al., 2018). However, the influence of these neurophysiological changes on the patient's cognitive abilities has not been extensively documented.

1.1. Glaucoma and Electrophysiology

Most electrophysiological measurements in patients with glaucoma are performed in the clinic (Bach and Poloschek, 2013; Senger et al., 2020), in order to evaluate electrical signals from the retina (i.e. an electroretinogram, ERG), the eye muscles (i.e. the electro-oculogram, EOG) or the visual cortex (i.e. visual evoked potentials, VEPs), (Vaegan and Hollows, 2006). VEPs are the electrophysiological responses recorded by two electrodes placed on the visual cortex (below the left and right occipital areas of the scalp) during the presentation of luminance or contrast changes over different parts of the visual field. According to Graham and Klistorner, half of all patients with glaucoma have abnormal VEP patterns (Graham and Klistorner, 1998). Kothari et al. studied the impact of the glaucoma stage (visual field loss) on VEP patterns in patients with POAG, (Kothari et al., 2014). The most affected patients had a longer latency for P100 (a positive potential recorded 100 ms after stimulus presentation). Although altered neuronal responses to low-level visual stimulation have been recorded in patients with glaucoma (Bach and Poloschek, 2013; Graham and Klistorner, 1998; Kothari et al., 2014; Senger et al., 2020; Vaegan and Hollows, 2006), neuronal changes in response to high-level visual stimulation tasks (i.e. those involving complex cognitive systems) have not previously been explored.

Functional electrophysiology can provide insights into the relationship between glaucoma and changes in brain dynamics and cognition. To the best of our knowledge, however, few studies have used electroencephalography (EEG) to measure brain activity in patients with glaucoma (Bola et al., 2015; Samanchi et al., 2021). Samanchi et al. measured spontaneous cortical activity under eyes-closed and eyes-open conditions in healthy controls and various populations of patients with glaucoma (Samanchi et al., 2021). Relative to controls, patients with POAG showed (i) significantly higher activity in the frontoparietal lobe in the eyes-closed condition, and (ii) significantly higher, more widespread activity in the frontal cortex and frontoparietal regions in the eyes-open condition. Samanchi et al. suggested that patients with POAG increased their spontaneous brain activity in response to nerve degeneration. However, possible changes in high-density EEG recordings and brain dynamics in response to external stimuli and cognitive tasks have not previously been studied in patients with glaucoma.

1.2. Visual cognition and semantic categorization in POAG

Visual semantic categorization has been investigated in patients with glaucoma (Lenoble et al., 2016; Roux-Sibilon et al., 2018). In low-contrast conditions, for example, patients with POAG were less able to categorize certain semantic categories (notably outdoor/indoor scenes(Roux-Sibilon et al., 2018) or for living/non living items (Lenoble et al. 2016)). Both studies highlighted impairment in the semantic categorization of low-contrast images viewed in the central visual field – a field that is relatively undamaged, according to static automated perimetry measurements. The hypothesis was that pathological degeneration of ganglion cells led notably to a worsening in the perception of coarse information, i.e. the overall perception of an object or a visual scene before the details are processed (the “coarse-to-fine” model), (Bullier, 2001; DeYoe and Van Essen, 1988; Parker et al., 1996; Petras et al., 2019; Peyrin et al., 2010).

The visual perception predictive coding models (Bar, 2007; Friston, 2005; Kauffmann et al., 2014) postulate that the brain constructs an internal representation of the external visual environment, which is used to generate ongoing predictions, anticipate visual sensory inputs, and facilitate recognition. According to operational studies (Kauffmann et al., 2015; Kveraga et al., 2007), the brain is suggested to generate continuous predictions by rapidly processing basic visual information, specifically low spatial frequencies. These predictions would subsequently influence slower visual processing, including the integration of high spatial frequencies. Numerous neuroimaging studies have documented functional and structural alterations in the brain as a result of the gradual degeneration of retinal ganglion cells (specifically magnocellular cells) in glaucoma, which can potentially impact cognitive functions (Frezzotti et al., 2016; Fukuda et al., 2018). Therefore, a recent study (Trouilloud et al., 2023) hypothesized that patients with glaucoma may not fully benefit from the predictive cortical mechanism involved in scene perception. Specifically, this mechanism entails the swift extraction of low spatial frequencies across the entire visual field, enabling the guidance of detailed perception in central vision. Their results revealed that patients with early glaucoma had greater semantic influence of low spatial frequencies on high spatial frequencies than controls, which then decreased for the severe cases of glaucoma. The authors reached the conclusion that the degradation of retinal ganglion cells has an impact on the processing of spatial frequencies in central vision. Studies investigating the categorization of coarse information (such as rapidly presented visual objects, low-contrast conditions, and low spatial frequencies) in healthy individuals have revealed that natural objects can be categorized using lower spatial frequencies compared to human-made objects. Non-living and human-made objects necessitate a different analysis involving the perception of fine details through higher spatial frequencies (Lenoble et al., 2013; Vannucci et al., 2001; Viggiano et

al., 2006). To date, there have been no studies evaluating whether patients with glaucoma exhibit the same visual dominance model for coarse information regarding natural objects.

In order to better understand the visual cognitive changes experienced by patients with glaucoma in their remaining vision, the current study investigate the processing and integration of spatial frequencies in central vision. Data were collected from participants during a semantic categorization task, measuring both behavioral and neurophysiological responses. The task involved categorizing natural and human-made visual objects using both low-pass filtered (LPF) and normal (non-filtered, NF) images. We hypothesized that changes in the overall perception of visual objects and in the related electrophysiological signals occurred in early-stage POAG (i.e. in patients whose central vision was clinically unaffected). Therefore, only patients with POAG and a recent-onset or moderate visual impairment were recruited. The patients' semantic categorization ability in a go/no-go task was compared with that of healthy, age-matched controls. Lastly, the EEG signal was recorded during the cognitive task, in order to assess the impact of glaucoma on high-level brain dynamics.

2. Materials and Methods

The experimental paradigm and the analysis were done based on the procedure described in (Wamain et al., 2023). A power analysis was conducted using the software G*Power (Faul et al., 2007) to determine the minimum sample size required. Statistical parameters were established based on prior published research (Lenoble et al., 2016), which demonstrated significant differences between glaucoma patients and healthy controls in behavioral data using the same experimental paradigm. Assuming a similar large effect size f = 0.60 for an ANOVA (fixed effects, special, main effects and interactions), an alpha error probability of 0.05, and a minimum power level (1-B) of 0.85: the total sample size was estimated at 28 participants across the two groups.

2.1. Participants

The study was conducted in the Ophthalmology Department at Claude Huriez Hospital (Lille, France). Fifteen patients (mean ± standard deviation age: 60.8 ± 10.6) and 15 healthy age-matched controls (mean age: 64.7 ± 6.84 years old) were recruited. A complete ophthalmological evaluation was performed for each participant, in order to confirm the diagnosis of POAG in the patient group and rule out any other complex visual disorders in both groups. All participants had to have a corrected binocular visual acuity of at least 0.1 Logarithm of the Minimum Angle of Resolution (logMAR) and contrast sensitivity higher than 1.65 Logarithm of the Contrast Sensitivity (Log CS) at the Pelli Robson. We excluded individuals with ophthalmologic complications (other than glaucoma for the glaucoma group) and a neurologic or psychiatric history (confirmation provided by the patient, supplemented by review of the hospital record). The clinical assessment prior to the experiment included a visual field evaluation using a 24-2 program Humphrey field analyzer (HFA) (Carl Zeiss Meditec Inc., Dublin, CA) for the patients and then a binocular visual acuity test and a binocular contrast sensitivity assessment (using the Pelli-Robson chart) for all participants. POAG was staged according to the mean deviation (MD) of the worst eye: 0.00 to -6.00 decibel (dB) for early POAG and -6.01 to -12.00 dB for moderate POAG. All the patients included in the experiment were considered to have a 0-5° central vision similar to the age-matched control group. Participants were assessed using the Mini Mental State Examination: a score of 25 or less was considered to indicate cognitive impairment (Folstein et al., 1975). The characteristics of the glaucomatous population are summarized in **Table 1.** Patients and controls did not differ in age and cognitive score (respectively, $p = 0.24$ and $p = 0.99$, student's t-test). The protocol was validated by the ethical committee of Lille (N°2016-4-S46) and a consent form was completed by each subject before their participation.

[Insert Table 1]

2.2. Materials

Using MATLAB software (version 2014b, MathWorks, Natick, MA, USA), we presented stimuli on a DELL (Dell inc., Austin, Texas, USA) S2721H screen (59.5° width at a distance of 57cm, resolution: 1920 x 1980 pixels; sampling rate: 75 Hz, brightness: 300 cd/m²). EEG data were recorded in a dimly illuminated room using a cap with 64 Ag/Agcl electrodes (BioSemi, Amsterdam, The Netherlands) mounted according to the 10-20 system over the whole scalp (http://www.biosemi.com). The EEG signals were acquired at a sampling rate of 512 Hz, using ActiView software (BioSemi). Four additional electrodes were placed to monitor eye movements, eye blinks (one electrode on the lateral canthi of the right eye, one below the right eye), and signals from mastoid sites (one electrode on each mastoid). The experiment began once the voltage differences between the electrodes were below 20 mV. The recordings of the presented images, EEG data, and keyboard responses were synchronized using a custom program developed with MATLAB and the Psychotoolbox (Brainard, 1997). Statistical analyses were performed with Jamovi software (Jamovi, 2020) and the threshold for statistical significance was set to $p<0.05$.

2.3. Stimuli

The stimuli were gray-scale 512 x 512 pixel photographs of 400 objects in four semantic categories: 100 images of animals, 100 images of furniture, 100 images of plants and 100 images of tools. The photographs were isolated from their original background for presentation on a gray screen. The luminance (mean ± standard deviation: 30.08 ± 1.45 cd/m²) and contrast (mean ± standard deviation Michelson contrast: 55% ± 0.8%) of the images were checked. There were no significant differences between the four semantic categories in the luminance or the contrast ($F_{3.297} = 2.48$, $p = 0.06$). The photographs were displayed so that they covered a visual angle 5° at the center of the screen; the fixed viewing distance of 57 cm was set by the use of a chinrest.

We built an NF version and an LPF version of each image, (**Figure 1A**). Each semantic category (animals, furniture, plants, and tools) therefore comprised 100 NF images and 100 LPF images. In the NF condition, pictures were displayed without spatial filtering. For the LPF condition, the Fourier transform of the NF version was multiplied by a Gaussian filter. Hence, the spatial frequency content above 3 cycles per degree of visual angle was removed.

[Insert Figure 1]

2.4. Procedure

After the participant had provided his/her written, informed consent, he/she was seated in an adjustable chair, and the EEG cap was installed. The experiment comprised two blocks of a go/no-go task: *Animal* and *Furniture.* The order of the *Animal* and the *Furniture* blocks was counterbalanced across the participants. For the *Animal* block, participants were instructed to press the space bar as soon as possible after the presentation of an animal target (200 stimuli: 100 NF and 100 LPF images). Participants were instructed not to press the space bar when a distractor appeared (200 images of plants and 200 images of tools = 400 in total). Within a given block, the probabilities of the NF and LPF conditions were equivalent. The same distractors were used in the *Furniture* block (600 images: 200 images of furniture, 200 images of tools, and 200 images of plants). Each participant performed a total of 1200 trials. The trial sequence began with the presentation of a central black fixation cross for 500 ms. The stimulus was then presented for 28 ms,(Lenoble et al., 2016; Macé et al., 2005) and the fixation cross reappeared for 2000 ms (the intertrial period) (**Figure 1B**).

2.5. Analyses

Only performance in target trials was considered in our analysis of behavioral and electrophysiological data. In order to compare the groups' respective level of performance, we focused on the effect of *object* (*Animals* vs. *Furniture*, i.e. the relationship between

performance and the visual object's semantic category) and the effect of *filter* (*NF* vs. *LPF*, i.e. the relationship between performance and the use of a low-pass filter).

2.5.1. Behavioral Data

Behavioral data were analyzed separately for each group (POAG vs. controls) and each condition (object and filter). We assessed three variables as a function of the processing level: accuracy, the decision criterion, and the response time. Accuracy and the decision criterion were calculated according to signal detection theory (Hautus et al., 2021; Stanislaw and Todorov, 1999). Four components were calculated: the hit rate (H, the percentage of trials in which a target was correctly detected), the correct rejection rate (CR, the percentage of distractor trials in which a manual response was not recorded), the miss rate (the percentage of missed targets), the false alarm rate (FA, the percentage of distractor trials in which a manual response was recorded). Accuracy was computed as the number of correct responses (hits and correct rejections) as a percentage of the total number of trials within a block. The response bias (i.e. the decision criterion (c)) for each participant was calculated as $[c = -\frac{1}{2}[z(H) + z(FA)]$ where z is the reverse normal distribution function (i.e. the z-score for a hit or an FA). A null decision criterion ($c=0$) corresponds to the absence of bias, a positive value ($c>0$) corresponds to conservative behavior with a tendency for "no-go" responses (the participant has more misses than FAs), and negative value ($c<0$) corresponds to conservative behavior with a tendency for "go" responses (the participant has more FAs than misses).

The tests used to assess inter- and intragroup differences depended on whether or not the data were normally distributed. The data on the participants' accuracy and decision criteria were not normally distributed ($p<0.05$ in the Shapiro-Wilk test); hence, intergroup differences were analyzed with a Kruskal-Wallis test, and intragroup differences were analyzed with a Friedman nonparametric analysis of variance (ANOVA) with repeated measures. Pairwise

comparisons were performed with the Durbin-Conover *post hoc* test. The response times were normally distributed ($p>0.05$ in the Shapiro-Wilk test). A parametric ANOVA with repeated measures was conducted on the mean latency of the participants' responses in the various conditions. Pairwise comparisons were performed *post hoc*, using the Bonferroni adjustment for type 1 errors.

2.5.2. Electrophysiological Data

Data were analyzed with the EEGLab toolbox (version 13.6.5b).(Delorme and Makeig, 2004) Two basic finite impulse response (FIR) filters were applied successively to continuous variables: a high-pass filter (order: 1691 points; transition band width: 1 Hz) and a low-pass filter (order: 227 points; transition band width: 7.5 Hz). Next, the filtered signal (1-30 Hz) was inspected visually, and periods with excessive numbers of noise artifacts were removed. Independent component analysis-based artifact correction was then used to correct for blink artifacts (Delorme et al., 2007). After the interpolation of noisy electrodes, the continuous EEG signal was re-referenced against the average reference signal (Delorme et al., 2015). Only data from target trials with a correct manual response were analyzed. Recordings were segmented in a time window of interest around the trial (from 200 ms before stimulus presentation to 1000 ms after the start of the stimulus presentation). Event-related potentials (ERPs) were built using the activity from -200 to 0 ms as the baseline (see Appendices, Figure A). After segmentation, the data were re-inspected visually by an expert EEG processing engineer in order to remove trials exhibiting muscle contraction artifacts (using ±100 μV as maximal deviation threshold. This final cleaning procedure removed 32% of data (range 22-40) leading to keep for subsequent analyze a minimum of 42 trials per condition (M= 68 trials per condition). Lastly, a Laplacian filter was used to increase the signal's spatial and temporal resolution (Perrin et al., 1989), and ERP data were then down-sampled to 100 Hz for submission to the classification analysis (Carlson et al., 2013).

2.5.3. Classifier

We used a data-driven approach to evaluate neural activation related to the effect of *object* (*Animals/Furniture*) and the effect of *filter* (NF/LPF). To this end, we adopted a classifier approach based on a naïve Bayesian implementation of linear discriminant analysis (Duda et al., 1974): this corresponds to the unsupervised training of an algorithm to categorize trials on the basis of the ERP patterns. Hence, this approach trained the classifier to recognize brain dynamic patterns evoked by the experimental conditions (*Object, Filter*). The algorithm required a training phase and a test phase. The classifier's performance was measured using 10-fold cross-validation (a training:test ratio of 9:1) for each individual dataset. For instance, the algorithm was trained on 9 subsets of one individual dataset so that it could classify the last subset, and the procedure was repeated ten times (so that each subset was classified once).

The classifier's sensitivity (i.e. decoding performance) was calculated for each participant as the mean accuracy over all trials for differentiating between neural responses (i.e. the response to an *Animal* trial vs. the response a *Furniture* trial) within the time window of interest (0 to 1000 ms). This decoding performance was computed as the mean decoding result for the trials, using a sliding window with three successive points (30 ms). The decoding performance at each time point was compared with chance (50%) in a Wilcoxon test. The p value was corrected for multiple comparisons by computing Benjamini and Hochberg's false discovery rate (FDR), (Benjamini and Hochberg, 1995).

Object and *filter* classifier analyses were used to test for effects on spatiotemporal brain dynamics. Moreover, we independently tested for the effects of *object* on performance, i.e. an *Animals* vs. *Furniture* analysis in NF trials and in LPF trials. The groups (POAG vs. controls) were compared with regard to the mean decoding performance. The difference in performance (computed using a Wilcoxon test) was defined as being statistically significant ($p<0.05$) or not over sliding periods of 30 ms. The classification results were used to model topographical

maps of brain activation during the semantic categorization of visual stimuli. Activation patterns were calculated according to Haufe et. al.'s method (Grootswagers et al., 2017; Haufe et al., 2014).

3. Results

3.1. Behavioral Data

Intragroup analyses of accuracy revealed an effect of *object* ($p<0.01$) and an effect of *filter* ($p<0.001$) in the age-matched controls (Durbin-Conover multiple comparisons, after a Friedman test [$\chi 2 = 30.6,\ df = 3;\ p < 0.01$]); whereas an effect of *filter* only ($p<0.05$) was observed for the patients with POAG. Both groups performed better in the NF condition than in the LPF condition. Regardless of the filter condition, the percentage of correct responses was higher for animal stimuli than for furniture stimuli (mean accuracy: 95% for *Animal* and 91% for *Furniture*; [$\chi 2 = 6.25,\ df = 1,\ p < 0.01$]; Friedman's test), (**Figure 2A**). Intergroup analyses showed that controls performed better than patients in the animal semantic category only (mean values: 95% vs. 91%, respectively [$\chi 2 = 5.3,\ df = 1,\ P = 0.02\ , \varepsilon^2 = 0.17$]; Kruskal-Wallis test), (**Figure 2A**). The two groups performed to a similar level with *Furniture* stimuli.

[Insert Figure 2]

A decision criterion analysis of the effect of *object* highlighted a conservative bias in both groups ($c > 0$, **Figure 2B**). Intragroup analyses demonstrated a significant *Animal* vs. *Furniture* difference in the decision criterion for controls (mean c = 0.28 for *Animal* vs. c = 0.53 for *Furniture*, [$\chi 2 = 8.00,\ df = 1,\ p < 0.01$]; Friedman test) but not for patients (mean c = 0.25 for *Animal* vs. 0.32 for *Furniture* [$\chi 2 = 0.28,\ df = 1,\ p = 0.59$]; Friedman test), (**Figure 2B**). Intergroup analyses showed that the decision criterion for *Animal* stimuli were similar in the two groups, whereas the conservative bias for *Furniture*

stimuli was greater in the control group than in the glaucoma group (mean c = 0.53 and 0.32, respectively [$\chi 2 = 5.2,\ \mathrm{df} = 1,\ \mathrm{p} = 0.02\ , \varepsilon^2 = 0.16$]; Kruskal-Wallis test).

The ANOVA of the response time revealed an effect of *object* for all participants ($F_{1.28} = 54.5$, $p<0.001$): *Furniture* stimuli had significantly longer response times (**Figure 2C)**. Indeed, the difference between *Furniture* stimuli and *Animal* stimuli during correct trials was significant for both controls (RT = 502 for *Animal* vs. $RT_{(F)}$ = 540 ms for *Furniture*; $p<0.001$) and patients (RT = 485 ms for *Animal* vs RT = 524 ms for *Furniture*, $p<0.001$). The effect of *filter* on response time was not significant ($F_{1.28} = 3.72$, $p = 0.06$), although responses were longer for *LPF* stimuli - especially in the *Furniture* semantic category. The intergroup difference was not significant ($F_{1.28} = 3.28$, $p = 0.08$), although response times were about 20 ms shorter for patients with glaucoma.

3.2. EEG data

The *Object* classifier was significantly more accurate than chance for classifying electrophysiological signals in *Animal* vs. *Furniture* trials, whereas the *Filter* classifier performed no better than chance (decoding performance = 0.5) for classifying electrophysiological signals in NF vs. LPF trials. We therefore focused our analyses of the EEG data on the *Object* classifier. Given the better behavioral performance in NF condition (i.e. for accuracy and the reaction time) in the two groups, we expected different brain dynamics of semantic categorization depending on the filter condition. Consequently, we compared effects in the groups, i.e. *Object* classifier performance in the NF condition (**Figure 3A**) and in LPF condition (**Figure 3B**).

[Insert Figure 3]

In the NF condition (**Figure 3A**), the difference between *Animal* and *Furniture* EEG signals (decoding performance) was significant in controls from 100 to 800 ms. This difference to be

appeared more transient and later in glaucomatous patients. The Wilcoxon test revealed two-time windows of interest in which patients and controls differed significantly ($p<0.05$) with regard to the decoding performance of the *Object* classifier: an early window from 70 to 170 ms after stimulus onset, and a late window from 400 to 600 ms.

3.2.1. Early processing

Classification between *Animal* and *Furniture* objects started at 150 ms in glaucoma group, i.e. around 50 ms later than in the control group. The topographic maps computed over this 70-170 ms time-window highlighted occipital activation in controls but not in patients with POAG.

3.2.2. Late processing

In the control group, a peak correct classification rate of 85% was observed between 400 and 600 ms; this corresponded to the greatest difference in neuronal responses between *Animals* and *Furniture*. This peak was not found in the POAG group, whose decoding performance was significantly lower than that of controls ($p<0.05$, Wilcoxon test). The topographic maps of the late component revealed frontal (blue) and parietal (red) activations in the control group. The activation patterns were less salient in the POAG group, with weak activity over the frontal and occipital regions.

In the LPF condition (**Figure 3B**), the brain dynamics were more similar in the two groups. The decoding performance significantly exceeded chance from 120 ms to 800 ms post-stimulus in controls, and from 170 ms to 800 ms in patients. The early processing interval was also present in patients but was not statistically significant. The decoding performance for controls remained high between 400 ms and 600 ms, although peak seen in the NF condition was absent. Patients were less sensitive throughout the late time window ($p<0.05$, Wilcoxon test). The topographic activation patterns were also more widely spread over the frontal and occipital regions in controls (i.e. much as seen in the patient group).

4. Discussion

The objective of this exploratory study was to assess behavioral and neurophysiological dynamics during a visuocognitive task in patients with POAG. To that end, a group of patients with early-stage POAG and a group of age-matched controls performed an ERP experiment in which they had to categorize briefly displayed visual objects (*Animal/Furniture* targets and *Plant/Tool* distractors) with different spatial frequencies (*NF/LPF*). Our results showed that patients with POAG were able to categorize visual objects on the basis of the overall shape. However, unlike the controls, the patients showed similar levels of accuracy in *Animal* trials and *Furniture* trials. The patient group applied the same decision criterion in each of the two semantic categories. Moreover, the behavioral and neurophysiological recordings highlighted POAG vs. control differences in brain dynamics during the semantic categorization task with central vision: the early stages of visual recognition were delayed for early-stage POAG participants, and this might have resulted in high-level cognitive compensation in the later part of the semantic categorization process.

On the behavioral level, our results showed that patients with POAG are able to categorize visual objects with a high level of performance under visually degraded condition. Firstly, we did not observe a difference in response time between controls and patients. This finding is in line with previous studies in which patients with glaucoma were able to perform complex cognitive tasks after brief exposure to stimuli (exposure time: 28 ms), (Lenoble et al., 2016). Moreover, in trials with correct responses, the two groups detected *Animals* more rapidly than *Furniture*. As suggested in the literature, visual object categorization triggers different behavioral responses depending on the animate vs. inanimate nature of the stimulus (Grootswagers et al., 2017). Secondly, the mean accuracy rate in the POAG group was high (90%). However, the POAG group's accuracy rates were similar for *Animal* stimuli and *Furniture* stimuli, whereas controls were significantly more accurate with *Animal* stimuli than

418 with *Furniture* stimuli. Hence, patients were significantly less accurate than controls when
419 categorizing *Animal* stimuli. We have two possible hypotheses for the lack of facilitation by
420 animate objects: (i) high-level cognitive impairment caused by neurophysiological damage to
421 the visual pathway (Boucard et al., 2009; Lawlor et al., 2018), and (ii) use of a different
422 response strategy (through compensation and cerebral re-organization), in an attempt to
423 maintain a good level of overall performance. The first hypothesis (the "damage" hypothesis)
424 was suggested by the fact that stimuli were displayed at a visual angle 0-5° in the central
425 visual field, which was known to be undamaged in the POAG group immediately prior to the
426 experiment. Consequently, the patients' low accuracy rate with *Animal* stimuli might be due
427 to changes in high-level brain areas beyond the primary visual cortex (Dai et al., 2013). This
428 result is also in line with an impairment of the coarse information processing and of the
429 predictive model in glaucoma (Roux-Sibilon et al., 2019): the progressive degradation of
430 ganglion cells impacts coarse information processing and fast predictive visual input that
431 facilitate perception of animate visual stimuli. The second hypothesis (the "compensation"
432 hypothesis) was prompted by our analysis of the *Furniture* data. Patients with POAG were as
433 accurate as controls during *Furniture* trials; they were not disadvantaged in categorizing
434 images of inanimate objects. Despite potential changes in their neuronal responses to
435 transiently displayed objects, patients maintained a good overall level of performance –
436 possibly by implementing a compensation strategy.

437 An analysis of the decision criterion during the task might be of value in determining which
438 of the two hypotheses is true. In the "go/no-go" task, errors correspond to oversights or FAs.
439 Oversights can be due to an attentional impairment and/or a conservative response bias (i.e.
440 the absence of a preferred response during ambiguous trials). FAs can be caused by impaired
441 inhibition during distractor trials and/or a liberal response bias (i.e. answering even during
442 ambiguous trials). Our group of patients applied the same decision criterion to all trials,

whereas controls demonstrated significantly more conservative behavior in *Furniture* trials (c= 0.53 in controls vs. 0.32 in glaucoma). Interestingly, these results highlighted a performance-impairing shift in decision strategy in controls (leading to more omissions of *Furniture* targets) but not in patients with POAG. The difference in the decision criterion in the control group (but not in the patient group) underpins the compensation hypothesis; it seems possible that in patients with glaucoma, the visual and decision-making systems adapt in order to maintain a neutral decision criterion and thus maximize the likelihood of detecting targets.

On the neurophysiological level, an analysis of temporal brain dynamics during visual and semantic category processing revealed two main differences between patients with POAG and age-matched controls: an early (visual) component (Martinovic et al., 2008; Di Russo et al., 2002) (70-170 ms) and a late (cognitive) component around 400 and 600 ms (Craddock et al., 2013). The key variable was decoding performance, i.e. time windows in which electrophysiological signals differed when comparing *Animal* trials with *Furniture* trials (i.e. the *object* classifier). During the two above-mentioned time windows, the classifier's decoding performance was significantly lower for patients than for controls. Moreover, in both NF and LPF conditions, the controls' classifier differentiated between *Animal* trial brain signals and *Furniture* trial brain signals as soon as 100 ms after the stimulus onset; this distinction occurred 50 ms later in the patient group. Our topographic analyses showed that over the 70 - 170 ms time window, the difference in *Animals* vs. *Furniture* activation was observed in the occipital region in controls but not in patients with POAG. These results are in line with literature reports (Graham and Klistorner, 1998; Kothari et al., 2014; Vaegan and Hollows, 2006) in which patients with glaucoma showed delayed early visual processing (relative to controls), as measured with VEPs and referred to as the P100 pattern. Here, using a cognitive task, we replicated the neurophysiological change under low-level visual

468 stimulation (i.e., contrast level shifts) reported in the literature. Furthermore, the late
469 component (a peak in decoding performance from 400 to 600 ms) was observed in the control
470 group but not in the POAG group. According to the literature (Craddock et al., 2013), late
471 activations in healthy subjects correspond to high-level processing and depend on the
472 semantic categorization task (the N350 component). The absence of the classification peak
473 and the presence of frontoparietal activation on the topographic map suggest that patients and
474 controls differed in the high-level information processing. Indeed, neural networks in the
475 frontal and prefrontal regions are known to be involved in decision making and can influence
476 the motor response (Gold and Shadlen, 2007; Paulus et al., 2001). In line with the
477 compensation hypothesis, the observed difference in this component may depend on the
478 behaviors present in controls but not in patients with glaucoma: i.e., the change in the decision
479 criterion only for the *Furniture* stimuli in controls. Our results on the early visual processing
480 delay and late cognitive changes are in line with the findings of a recent functional MRI
481 study: functional reorganization was not observed in the primary visual cortex, whereas there
482 were significant changes in the activation of top-down networks from the frontal regions to
483 the visual cortex (Prabhakaran et al., 2021). Prabhakaran et al.'s study of the functional
484 dynamics of V1 in glaucoma highlighted aberrant activation within the lesion projection zone
485 (corresponding to the projection of the visual field's scotomas in V1) and top-down
486 modulations from higher cortical areas. Further brain imaging studies in patients with
487 glaucoma are needed to replicate these findings and characterize the nature of cortical
488 plasticity in areas beyond the visual cortex.

489 The present study had some limitations. First, the number of participants per group was
490 relatively small. However, we are confident that this should not significantly affect our
491 conclusions on behavioral data and neurophysiological data because we employed a common
492 and robust experimental paradigm and calculated the effect size based on previous findings in

493 POAG patient in the same task (Lenoble et al., 2016). Additionally, the task included 1200
494 trials to obtain reliable individual EEG signals. Nevertheless, due to the sample size of the
495 patient group and the limitation to early POAG, we were unable to assess the impact of visual
496 impairment on behavioral performance. A larger cohort of patients would allow to examine
497 different stages of glaucoma and to provide valuable insights to validate or invalidate the
498 compensation hypothesis in our results. Second, we did not observe the effect of the spatial
499 frequency *filter* on the behavioral and neurophysiological data. We measured overall shape
500 perception ability by adapting the methods described in (Macé et al., 2005) and (Lenoble et
501 al., 2016): the stimuli were flashed up as black and white images for 28 ms. According to
502 Lenoble et al., patients with glaucoma presented longer response times and lower correct
503 response rates at a medium contrast level (50%), relative to age-matched controls performing
504 the same semantic categorization task (Lenoble et al., 2016). Moreover, the degradation of
505 retinal ganglion cells is known to reduce sensitivity to low spatial frequencies in glaucoma
506 (McKendrick et al., 2007), impacting the anticipation of visual sensory input in central vision
507 according to predictive coding models (Kveraga et al., 2007; Trouilloud et al., 2023). Thus,
508 we expected the patients' level of performance to be (i) lower in the LPF condition than in the
509 NF condition and (ii) lower than with controls. In fact, both groups of participants had
510 difficulty in the LPF condition; this difficulty did not therefore appear to be specific for the
511 visual deficit – except with *Animal* stimuli. Similarly, the classifier was not able to
512 discriminate between NF trials and LPF trials by reference to the brain dynamics. One
513 possible explanation is that the NF condition corresponded to a *coarse* display of stimuli,
514 given (i) the brief presentation (28 ms), the small size, and the lack of specific information for
515 central vision (e.g. color information). Further comparisons of a low-pass filter (LPF) vs. a
516 high spatial frequency filter (rather than no filter) might shed light on differences in
517 information processing between healthy controls and patients with POAG as a function of the

spatial frequency. Additionally, these comparisons could allow us to identify distinct brain dynamic profiles in a classification analysis.

5. Conclusion

Our study provided preliminary information on high-level visual functions and brain dynamics in patients with POAG. We found that the patients and healthy controls differed in their ability to categorize overall perceptions of visual objects. Controls (but not patients with POAG) performed better when categorizing *Animal* stimuli. Glaucoma impacted overall shape perception for visual objects and weakened the facilitating effect of LSF information. On the neurophysiological level, the patients' brain responses differ from those of the controls in early and late time windows. Even though caution must be exerted when comparing behavioral and neurophysiological analyses, our results suggested that (i) the early stages of visual processing were impaired in patients with POAG, and (ii) higher-level compensation was required to categorize visual objects with degraded properties. Thus, the neuroanatomical changes observed in previous brain imaging studies might be related not only to impairments in the early stages of perception but also to structural plasticity and compensation mechanisms beyond the primary visual cortex. Further visuo-cognitive studies, involving a larger cohort of patients with varying stages of glaucoma from early to severe, are essential to investigate the interplay between visual impairment, neurological changes, and compensatory behaviors.

References

Arrigo A, Aragona E, Saladino A, Arrigo D, Fantaguzzi F, Battaglia Parodi M, et al. Cognitive Dysfunctions in Glaucoma: An Overview of Morpho-Functional Mechanisms and the Impact on Higher-Order Visual Function. Front Aging Neurosci 2021;13:1–13. https://doi.org/10.3389/fnagi.2021.747050.

Bach M, Poloschek CM. Electrophysiology and glaucoma: Current status and future challenges. Cell Tissue Res 2013;353:287–96. https://doi.org/10.1007/s00441-013-1598-6.

Bar M. The proactive brain: using analogies and associations to generate predictions. Trends Cogn Sci 2007;11:280–9. https://doi.org/10.1016/j.tics.2007.05.005.

Benjamini Y, Hochberg Y. Controlling the False Discovery Rate: A Practical and Powerful Approach to Multiple Testing. Journal of the Royal Statistical Society: Series B (Methodological) 1995;57:289–300. https://doi.org/10.1111/j.2517-6161.1995.tb02031.x.

Bola M, Gall C, Sabel BA. Disturbed temporal dynamics of brain synchronization in vision loss. Cortex 2015. https://doi.org/10.1016/j.cortex.2015.03.020.

Boucard CC, Hernowo AT, Maguire RP, Jansonius NM, Roerdink JBTM, Hooymans JMM, et al. Changes in cortical grey matter density associated with long-standing retinal visual field defects. Brain 2009;132:1898–906. https://doi.org/10.1093/brain/awp119.

Brainard DH. The Psychophysics Toolbox. Spat Vis 1997;10:433–6.

Bullier J. Integrated model of visual processing. Brain Res Rev 2001;36:96–107. https://doi.org/10.1016/S0165-0173(01)00085-6.

Carlson T, Tovar DA, Alink A, Kriegeskorte N. Representational dynamics of object vision: The first 1000 ms. J Vis 2013;13:1–19. https://doi.org/10.1167/13.10.1.

Chen WW, Wang N, Cai S, Fang Z, Yu M, Wu Q, et al. Structural Brain Abnormalities in Patients with Primary Open-Angle Glaucoma: A Study with 3T MR Imaging. Investigative Opthalmology & Visual Science 2013;54:545. https://doi.org/10.1167/iovs.12-9893.

Craddock M, Martinovic J, Müller MM. Task and Spatial Frequency Modulations of Object Processing: An EEG Study. PLoS One 2013;8:1–12. https://doi.org/10.1371/journal.pone.0070293.

Dai H, Morelli JN, Ai F, Yin D, Hu C, Xu D, et al. Resting-state functional MRI: Functional connectivity analysis of the visual cortex in primary open-angle glaucoma patients. Hum Brain Mapp 2013;34:2455–63. https://doi.org/10.1002/hbm.22079.

Delorme A, Makeig S. EEGLAB: an open source toolbox for analysis of single-trial EEG dynamics including independent component analysis. J Neurosci Methods 2004;134:9–21. https://doi.org/10.1016/j.jneumeth.2003.10.009.

Delorme A, Miyakoshi M, Jung T-P, Makeig S. Grand average ERP-image plotting and statistics: A method for comparing variability in event-related single-trial EEG activities across subjects and conditions. J Neurosci Methods 2015;250:3–6. https://doi.org/10.1016/j.jneumeth.2014.10.003.

574 Delorme A, Sejnowski T, Makeig S. Enhanced detection of artifacts in EEG data using
575 higher-order statistics and independent component analysis. Neuroimage 2007;34:1443–9.
576 https://doi.org/10.1016/j.neuroimage.2006.11.004.

577 DeYoe EA, Van Essen DC. Concurrent processing streams in monkey visual cortex. Trends
578 Neurosci 1988;11:219–26. https://doi.org/10.1016/0166-2236(88)90130-0.

579 Duda RO, Hart PE, Stork DG. Pattern Classification and Scene Analysis. vol. 3. 1974.
580 https://doi.org/10.2307/2344977.

581 Faul F, Erdfelder E, Lang A-G, Buchner A. G*Power 3: A flexible statistical power analysis
582 program for the social, behavioral, and biomedical sciences. Behav Res Methods
583 2007;39:175–91. https://doi.org/10.3758/BF03193146.

584 Folstein MF, Folstein SE, McHugh PR. "Mini-mental state" - A pratical method for grading
585 the cognitive state of patients for the clinician. J Psychiatr Res 1975;12:189–98.
586 https://doi.org/10.1016/0022-3956(75)90026-6.

587 Frezzotti P, Giorgio A, Toto F, De Leucio A, De Stefano N. Early changes of brain
588 connectivity in primary open angle glaucoma. Hum Brain Mapp 2016;37:4581–96.
589 https://doi.org/10.1002/hbm.23330.

590 Friston K. A theory of cortical responses. Philosophical Transactions of the Royal Society B:
591 Biological Sciences 2005;360:815–36. https://doi.org/10.1098/rstb.2005.1622.

592 Fukuda M, Omodaka K, Tatewaki Y, Himori N, Matsudaira I, Nishiguchi KM, et al.
593 Quantitative MRI evaluation of glaucomatous changes in the visual pathway. PLoS One
594 2018;13:e0197027. https://doi.org/10.1371/journal.pone.0197027.

595 Gold JI, Shadlen MN. The neural basis of decision making. Annu Rev Neurosci 2007;30:535–
596 74. https://doi.org/10.1146/annurev.neuro.29.051605.113038.

597 Graham SL, Klistorner A. Electrophysiology: A review of signal origins and applications to
598 investigating glaucoma. Aust N Z J Ophthalmol 1998;26:71–85.
599 https://doi.org/10.1046/j.1440-1606.1998.00082.x.

600 Grootswagers T, Ritchie JB, Wardle SG, Heathcote A, Carlson TA. Asymmetric Compression
601 of Representational Space for Object Animacy Categorization under Degraded Viewing
602 Conditions. J Cogn Neurosci 2017;29:1995–2010. https://doi.org/10.1162/jocn_a_01177.

603 Haufe S, Meinecke F, Görgen K, Dähne S, Haynes JD, Blankertz B, et al. On the
604 interpretation of weight vectors of linear models in multivariate neuroimaging. Neuroimage
605 2014;87:96–110. https://doi.org/10.1016/j.neuroimage.2013.10.067.

606 Hautus MJ, Macmillan NA, Creelman CD. Detection Theory. 2nd ed. New York: Routledge;
607 2021. https://doi.org/10.4324/9781003203636.

608 Jamovi. The jamovi project 2020:(Version 1.2) [Computer Software].
609 https://doi.org/https://www.jamovi.org.

610 Kauffmann L, Chauvin A, Pichat C, Peyrin C. Effective connectivity in the neural network
611 underlying coarse-to-fine categorization of visual scenes. A dynamic causal modeling study.
612 Brain Cogn 2015;99:46–56. https://doi.org/10.1016/j.bandc.2015.07.004.

613 Kauffmann L, Ramanoel S, Peyrin C. The neural bases of spatial frequency processing during
614 scene perception. Front Integr Neurosci 2014;8. https://doi.org/10.3389/fnint.2014.00037.

615 Kothari R, Bokariya P, Singh R, Singh S, Narang P. Correlation of pattern reversal visual
616 evoked potential parameters with the pattern standard deviation in primary open angle
617 glaucoma. Int J Ophthalmol 2014;7:326–9. https://doi.org/10.3980/j.issn.2222-
618 3959.2014.02.24.

619 Kveraga K, Boshyan J, Bar M. Magnocellular Projections as the Trigger of Top-Down
620 Facilitation in Recognition. The Journal of Neuroscience 2007;27:13232–40.
621 https://doi.org/10.1523/JNEUROSCI.3481-07.2007.

622 Lawlor M, Danesh-Meyer H, Levin LA, Davagnanam I, De Vita E, Plant GT. Glaucoma and
623 the brain: Trans-synaptic degeneration, structural change, and implications for
624 neuroprotection. Surv Ophthalmol 2018. https://doi.org/10.1016/j.survophthal.2017.09.010.

625 Lenoble Q, Bordaberry P, Rougier M-B, Boucart M, Delord S. Influence of Visual Deficits on
626 Object Categorization in Normal Aging. Exp Aging Res 2013;39:145–61.

627 Lenoble Q, Lek JJ, McKendrick AM. Visual object categorisation in people with glaucoma.
628 British Journal of Ophthalmology 2016;100:1585–90. https://doi.org/10.1136/bjophthalmol-
629 2015-308289.

630 Macé MJM, Thorpe SJ, Fabre-Thorpe M. Rapid categorization of achromatic natural scenes:
631 How robust at very low contrasts? European Journal of Neuroscience 2005;21:2007–18.
632 https://doi.org/10.1111/j.1460-9568.2005.04029.x.

633 Martinovic J, Gruber T, Müller MM. Coding of visual object features and feature
634 conjunctions in the human brain. PLoS One 2008;3.
635 https://doi.org/10.1371/journal.pone.0003781.

636 McKendrick AM, Sampson GP, Walland MJ, Badcock DR. Contrast Sensitivity Changes Due
637 to Glaucoma and Normal Aging: Low-Spatial-Frequency Losses in Both Magnocellular and
638 Parvocellular Pathways. Investigative Opthalmology & Visual Science 2007;48:2115.
639 https://doi.org/10.1167/iovs.06-1208.

640 Nucci C, Garaci F, Altobelli S, Di Ciò F, Martucci A, Aiello F, et al. Diffusional Kurtosis
641 Imaging of White Matter Degeneration in Glaucoma. J Clin Med 2020;9:3122.
642 https://doi.org/10.3390/jcm9103122.

643 Nuzzi R, Dallorto L, Rolle T. Changes of Visual Pathway and Brain Connectivity in
644 Glaucoma: A Systematic Review. Front Neurosci 2018;12.
645 https://doi.org/10.3389/fnins.2018.00363.

646 Parker DM, Lishman JR, Hughes J. Role of coarse and fine spatial information in face and
647 object processing. J Exp Psychol Hum Percept Perform 1996;22:1448–66.
648 https://doi.org/10.1037/0096-1523.22.6.1448.

649 Paulus MP, Hozack N, Zauscher B, McDowell JE, Frank L, Brown GG, et al. Prefrontal,
650 parietal, and temporal cortex networks underlie decision-making in the presence of
651 uncertainty. Neuroimage 2001;13:91–100. https://doi.org/10.1006/nimg.2000.0667.

Perrin F, Pernier J, Bertrand O. Spherical splines for scalp potential and current density mapping 10.1016/0013-4694(89)90180-6 : Electroencephalography and Clinical Neurophysiology | ScienceDirect.com. ElectroencephaJography and Clinical Neurophysiology 1989;72:184–7.

Petras K, Oever S ten, Jacobs C, Goffaux V. Coarse-to-fine information integration in human vision. Neuroimage 2019;186:103–12. https://doi.org/10.1016/j.neuroimage.2018.10.086.

Peyrin C, Michel CM, Schwartz S, Thut G, Seghier M, Landis T, et al. The Neural Substrates and Timing of Top-Down Processes during Coarse-to-Fine Categorization of Visual Scenes: A Combined fMRI and ERP Study. J Cogn Neurosci 2010;22:2768–80. https://doi.org/10.1162/jocn.2010.21424.

Prabhakaran GT, Al-Nosairy KO, Tempelmann C, Wagner M, Thieme H, Hoffmann MB. Functional Dynamics of Deafferented Early Visual Cortex in Glaucoma. Front Neurosci 2021;15:1–13. https://doi.org/10.3389/fnins.2021.653632.

Roux-Sibilon A, Rutgé F, Aptel F, Attye A, Guyader N, Boucart M, et al. Scene and human face recognition in the central vision of patients with glaucoma. PLoS One 2018;13:e0193465. https://doi.org/10.1371/journal.pone.0193465.

Roux-Sibilon A, Trouilloud A, Kauffmann L, Guyader N, Mermillod M, Peyrin C. Influence of peripheral vision on object categorization in central vision. J Vis 2019;19:7. https://doi.org/10.1167/19.14.7.

Di Russo F, Martínez A, Sereno MI, Pitzalis S, Hillyard SA. Cortical sources of the early components of the visual evoked potential. Hum Brain Mapp 2002;15:95–111. https://doi.org/10.1002/hbm.10010.

Samanchi R, Prakash Muthukrishnan S, Dada T, Sihota R, Kaur S, Sharma R. Altered spontaneous cortical activity in mild glaucoma: A quantitative EEG study. Neurosci Lett 2021;759:136036. https://doi.org/10.1016/j.neulet.2021.136036.

Senger C, Moreto R, Watanabe SES, Matos AG, Paula JS. Electrophysiology in Glaucoma. J Glaucoma 2020;29:147–53. https://doi.org/10.1097/IJG.0000000000001422.

Stanislaw H, Todorov N. Calculation of signal detection theory measures. Behavior Research Methods, Instruments, & Computers 1999;31:137–49. https://doi.org/10.3758/BF03207704.

Trouilloud A, Ferry E, Boucart M, Kauffmann L, Warniez A, Rouland J-F, et al. Impact of glaucoma on the spatial frequency processing of scenes in central vision. Vis Neurosci 2023;40:E001. https://doi.org/10.1017/S0952523822000086.

Vaegan, Hollows FC. Visual-evoked response, pattern electroretinogram, and psychophysical magnocellular thresholds in glaucoma, optic atrophy, and dyslexia. Optometry and Vision Science 2006. https://doi.org/10.1097/01.opx.0000225920.97380.62.

Vannucci M, Viggiano MP, Argenti F. Identification of spatially filtered stimuli as function of the semantic category. Cognitive Brain Research 2001;12:475–8. https://doi.org/10.1016/S0926-6410(01)00086-6.

690 Viggiano MP, Righi S, Galli G. Category-specific visual recognition as affected by aging and
691 expertise. Arch Gerontol Geriatr 2006;42:329–38.
692 https://doi.org/10.1016/j.archger.2005.08.003.

693 Wamain Y, Garric C, Lenoble Q. Dynamics of low-pass-filtered object categories: A
694 decoding approach to ERP recordings. Vision Res 2023;204:108165.
695 https://doi.org/10.1016/j.visres.2022.108165.

696

697

Figure's legends

Table 1: Demographic and clinical characteristics of the patients with primary open-angle glaucoma (POAG). MMSE: Mini Mental State Examination; logMAR: Logarithm of the Minimum Angle of Resolution; Log CS: Logarithm of the Contrast Sensitivity; HFA MD: Humphrey field analyzer mean deviation; dB: decibel; NA: Non-Applicable.

Figure 1 : Stimuli and procedure. (A) Examples of stimuli from two semantic categories (Animals and Furniture) in the nonfiltered condition (NF) and the low-pass-filtered condition (LPF: spatial frequencies above 3 cycles per degree had been removed). **(B) The experimental sequence:** a black fixation cross appeared for 500 milliseconds (ms). The stimulus was then displayed for 28 ms. The participant has been instructed to press the space bar as soon as possible during the intertrial period of 2000 ms only when a target (an animal or furniture) had been displayed.

Figure 2: An intergroup comparison and the effect of object for semantic categorization performance: Accuracy (**A**), decision criterion (**B**) and response time (**C**). Accuracy corresponds to the percentage of correct detections and correct rejections. The decision criterion corresponds to the response bias and ranges from neutral (c=0) to conservative (c > 0). The response time corresponds to the time interval (in ms) between presentation of the stimulus and the manual response (in correct trials only). Group average performances are plotted as a function of the Animal condition or the Furniture condition on the horizontal axes. The control and glaucoma groups are represented in blue and orange, respectively. Error bars correspond to 95% confidence intervals. *** $p<0.001$, ** $p<0.01$, * $p<0.05$.

Figure 3: Object decoding (based on the EEG signal) in the non-filtered (NF) condition (A) and the low-pass filtered (LPF) condition (B). The graphs show the change over time in the classifier's decoding performance for Animal vs. Furniture neuronal responses, as a function of the participant group (glaucoma in green and controls in blue). Shaded areas correspond to the group's standard error. Green and blue stars indicate significant differences in decoding performance (vs. chance, shown by the grey line). Black stars indicate significant differences between the Glaucoma and control groups (Wilcoxon test, $p<0.05$). The lower panels are the corresponding topographic activation maps for the scalp regions involved in object classification in specific time windows (1: early processing, 70-170 ms; 2: late processing, 400-600 ms). Green areas represent areas that are neutral in the classification task, whereas blue and red areas represent polarized activation patterns of

importance in the classification task. The view corresponds to the top of the head, with the nose pointing towards the top of the page (top-frontal, middle-parietal, bottom-occipital).

Table

Table 1: Demographic and clinical characteristics of the participants. MMSE: Mini Mental State Examination; logMAR: Logarithm of the Minimum Angle of Resolution; Log CS: Logarithm of the Contrast Sensitivity; HFA MD: Humphrey field analyzer mean deviation; dB: decibel; NA: Non-Applicable; Sex (F=Female, M=Male).

Participants	*Sex*	*Age (years)*	*MMSE (out of 30)*	*Binocular visual acuity (logMAR)*	*Contrast sensitivity (log CS)*	*Worst-eye HFA MD (dB)*	*Glaucoma stage*
Patients with POAG							
G1	F	56	30	0.10	1.85	-4.6	Early
G2	M	82	27	0.00	1.85	-4.7	Early
G3	M	69	29	0.10	2	-3.6	Early
G4	M	56	27	0.00	1.7	-6.35	Moderate
G5	F	66	29	0.00	1.85	-7.4	Moderate
G6	F	61	28	0.10	1.7	-2.9	Early
G7	M	70	27	0.10	1.7	-3.4	Early
G8	F	60	27	0.00	2	-1.3	Early
G9	F	65	28	0.10	1.7	-8.4	Moderate
G10	F	69	30	0.00	1.85	-1.9	Early
G11	M	53	27	0.00	1.85	-3.6	Early
G12	M	43	29	0.00	2	-1	Early
G13	M	43	28	0.00	2	-1.2	Early
G14	M	67	27	0.00	1.85	-3.7	Early
G15	M	52	28	0.10	1.7	-2	Early
Age-matched Controls				≥ 0.10	> 1.65	NA	NA
C1	M	53	30	-	-	-	-
C2	F	76	28	-	-	-	-
C3	M	76	29	-	-	-	-
C4	M	62	28	-	-	-	-
C5	M	67	29	-	-	-	-
C6	F	75	30	-	-	-	-
C7	F	63	27	-	-	-	-
C8	M	63	28	-	-	-	-
C9	F	61	27	-	-	-	-
C10	F	60	30	-	-	-	-
C11	M	65	26	-	-	-	-
C12	M	58	25	-	-	-	-
C13	F	60	30	-	-	-	-
C14	M	70	28	-	-	-	-
C15	F	62	26	-	-	-	-

735 **Figure 1**

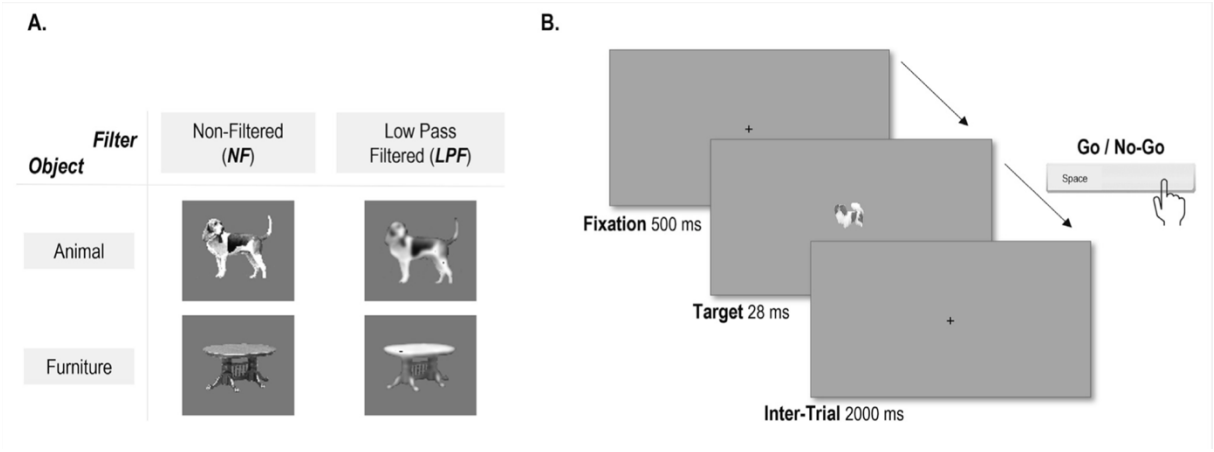

736

737

Figure 2

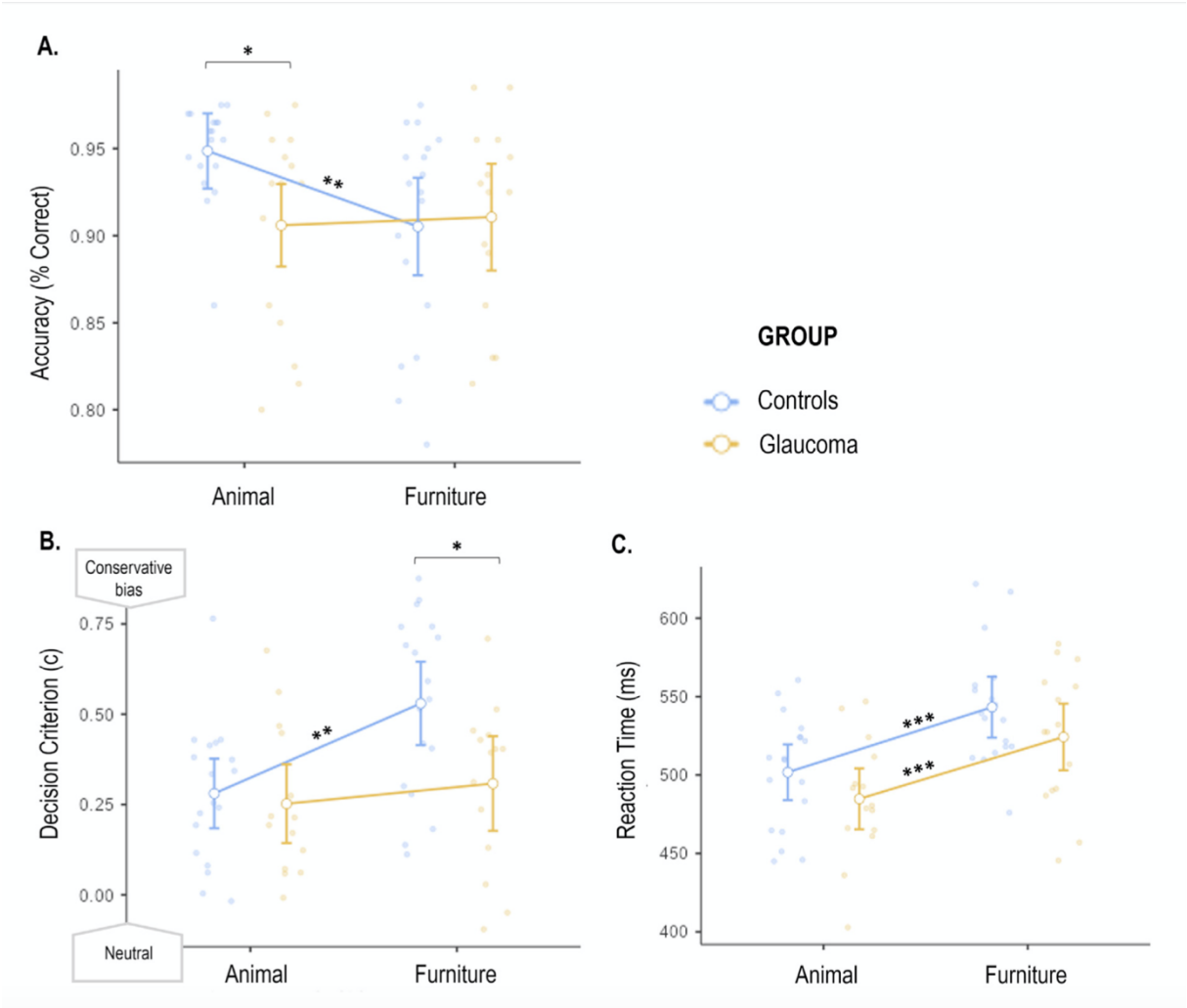
A.
Accuracy (% Correct)
0.95
0.90
0.85
0.80
*
**
Animal
Furniture
GROUP
Controls
Glaucoma
B.
Conservative bias
Neutral
Decision Criterion (c)
0.75
0.50
0.25
0.00
*
**
Animal
Furniture
C.
Reaction Time (ms)
600
550
500
450
400
***
***
Animal
Furniture

741 **Figure 3**

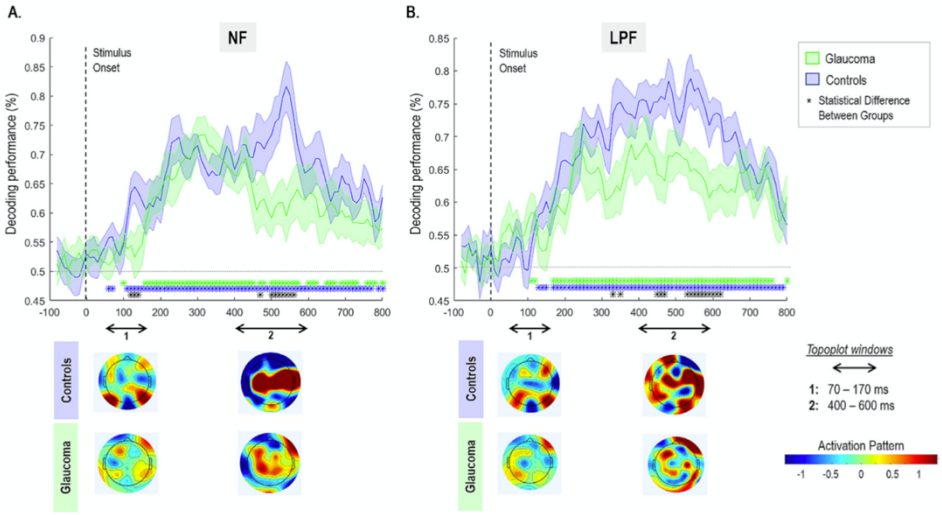

742